Microglial Activation in Rat Experimental Spinal Cord Injury Model

Alireza Abdanipour[1], Taki Tiraihi[*2,3], Taher Taheri[3] and Hadi Kazemi[3]

[1]*Stem Cells Research Laboratory, Department of Medical Science, Ardabil Branch, Islamic Azad University, Ardabil, Iran;* [2]*Dept. of Anatomical Sciences, School of Medical Sciences, Tarbiat Modares University, Tehran, Iran;* [3]*Shafa Neurosciences Research Center, Khatam Al-Anbia Hospital, Tehran, Iran*

ABSTRACT

Background: The present study was designed to evaluate the secondary microglial activation processes after spinal cord injury (SCI). **Methods:** A quantitative histological study was performed to determine ED-1 positive cells, glial cell density, and cavitation size in untreated SCI rats at days 1, 2, and 4, and weeks 1, 2, 3, and 4. **Results:** The results of glial cell quantification along the 4900-µm long injured spinal cord showed a significant increase in glial cell density percentage at day 2 as compared to other days. Whereas the highest increase in ED-1 immunoreactive cells (monocyte/phagocyte marker in rats) was observed at day 2 (23.15%) post-injury. Evaluation of cavity percentage showed a significant difference between weeks 3 and 4 post-injury groups. **Conclusions:** This study provides a new insight into the multiphase immune response to SCI, including cellular inflammation, macrophages/microglia activation, glial cell density, and cavitation. Better understanding of the inflammatory processes associated with acute SCI would permit the development of better therapeutic strategies. *Iran. Biomed. J. 17 (4): 214-220, 2013*

INTRODUCTION

Spinal cord injury (SCI) is one of the major disabilities requiring more effective treatments [1]. Understanding the molecular events underlying SCI can provide useful information for developing novel therapeutic strategies for human clinical trials [2]. Pathophysiology of SCI is characterized by robust immune response, activation of various cytokines, damage to blood-spinal cord barrier, myelin loss as well as axonal degradation, cell death, and functional deficit [3-5].

The early phase of inflammatory response in SCI is initiated by migration of peripherally derived immune cells into the lesion site [6], where the ED-1 positive cells are present [7, 8]. ED-1 is an intracellular antigen found in activated resident microglia, macrophages and monocytes in rats. Resting microglia/macrophages in the central nervous system is recognized by their distinct star-shaped morphology and positivity only for OX42, a type I transmembrane protein found on monocytes, macrophages, granulocytes, some B cells, dendritic cells, and natural killer cells.

In contrast, activated phagocytic microglias are rounded and therefore not easily distinguishable from peripheral macrophages [9]. Moreover, the lesion site contains large number of apoptotic and necrotic neurons, and glial cells are typically present at the center of the site [10].

This study was designed to evaluate the immunoreactivity of ED-1 positive cells, density of glial cells, and cavitation in untreated SCI of the rats at different time points (days 1, 2, and 4 and weeks 1, 2, 3, and 4) after SCI.

MATERIALS AND METHODS

Contusion rat SCI model. Female Sprague-Dawley rats (250–350 g; Razi Institute for Serums and Vaccines, Tehran, Iran) were housed under standard conditions. All procedures were approved by the Animal Care and Use Committee of Tarbiat Modares University (Tehran, Iran). Rats were randomly assigned to 7 experimental groups (n = 6 for each group) as follows: (1) day 1, (2) day 2, (3) day 4, (4)

*Corresponding Author; Fax: (+98-21) 801 6544; E-mail: takialtr@modares.ac.ir or ttiraihi@gmail.com

week 1, (5) week 2, (6 and 7) weeks 3 and 4 post SCI. Contusion model of SCI was performed using a standard procedure [11]. Briefly, the rats were anesthetized with an intraperitoneal injection of 80 mg/kg ketamine and 5 mg/kg xylazine. The dorsal region of the rats was shaved, and laminectomy was performed at the T12-L1 level. The exposed spinal cord was injured using a 10-g metal rod with a 2-mm diameter, dropped from a 25-mm height [12]. After the surgery, the animals were recovered by subcutaneous injection of 10 ml lactated Ringer's solution. One-week post-operative care included manual bladder expression and intramuscular injection of 50 mg/kg cefazolin (Jabir Ibn Hayan, Tehran, Iran) [13].

Histopathological quantitative analysis. For histopathological analysis, rats were sacrificed at the assigned time points (listed above) and perfused transcardially with 4% paraformaldehyde in PBS for 5 minutes. The lesion area was removed and post-fixed in 4% paraformaldehyde for another 12 hours. Next, the tissues were processed using an automatic processor (Leica TP 1020: Leica Microsystems, Wetzlar, Germany) and embedded in paraffin. To assess the glial cell density per area and cavity percentage, serial sections (thickness 7 μm) were prepared. The sections were then dewaxed with chloroform and stained with hematoxylin and eosin (H & E) [14]. Total tissue and cavity volume (mm^3) of 4900-μm long of the spinal cord (including rostral and caudal regions from the injury epicenter) were assessed for each sample by using Image J 1-44 software (NIH, USA). Cavity percentage and spared tissue were calculated for 35 sections by using the Cavalieri's method [15] (equation 1: a, measured area and d, intersection distance). Serial summation of the spared tissue and cavity volumes yielded the total volume of the spared tissue. Any necrotic tissue within the cavities was counted as a part of the lesion; any small cavity was also calculated. Somata size of glial cells (approximately 8-2 μm) was used for evaluating numerical density per area [16, 17]. Equation 2 was used for determining of cell density, (N: number of objects counted, A: area and δ: effective depth of field) [18].

Equation 1: $V_{sp} = a \times d$

Equation 2: $D = \dfrac{N}{A\delta}$

For immunostaining, sections were dewaxed in chloroform and further hydrated using graded ethanol (100%, 96%, 90%, and 70%) and distilled water. The sections were then immersed in 0.3% hydrogen peroxide in methanol at 20°C for 10 minutes to inactivate endogenous peroxidase. Next, the sections were preincubated in a blocking solution (10% swine serum in (Tris-buffered saline/BSA at room temperature for 15 minutes, after which they were incubated in primary antibody at 4°C overnight (1:100 dilution; anti-ED-1 monoclonal mouse IgG; Serotec, Oxford, UK). Next, the sections were mounted with avidin and biotinylated horseradish peroxidase (ABC kit; Vector Labs, Burtingame, CA, USA), and antigen was detected using the diaminobenzidine method. For counterstaining, the sections were stained with hematoxylin. Immunostaining was performed on 6 7-μm sections from each animal (2 sections from the rostral, central and caudal areas). Then, 5 fields were studied at 20×, including both ventral horns, both dorsal horns, and a central canal region. For evaluating SCI, the immunoreactivity of ED-1 cells and percentage of brown pixels per area were determined (stained with peroxidase) using the Image J software.

Statistics. All the statistical analyses were performed using SPSS (release 15) software (www.ibm.com/ software/ analytics/spss/). All data are presented as mean and standard error of mean (SEM). One-way ANOVA, followed by Tukey's post hoc comparison test, was used to compare multiple means within groups. *P* value <0.05 was considered statistically significant.

RESULTS

Evaluation of ED-1 immunoreactivity during 28 days after the injury. For evaluating microglial and macrophage activation, ED-1 (a lysosomal marker) immunostaining was performed and Image J was used to analyze results by comparing pixel density per area. In this study, ED-1 positive cells were evaluated in SCI rats at days 1, 2, and 4, and weeks 1, 2, 3, and 4) after SCI. Moreover, we noticed that ED-1 positive cells appeared to be more dispersed in the first week than other time points (Fig. 1). A significant difference was observed between the day 2 group (23.15% ± 0.94 of positive pixels per area) and the other groups (day 1: 13.69% ± 1.58 and week 1: 20.33% ± 1.52 of positive pixels per area). The highest increase in ED-1 immunoreactive cells was observed between 2 and 4 days post injury. Data analyses are shown in Figure 2.

Evaluation of glial cell density. Histological assessments were performed on H & E-stained sections during 28 days to evaluate the mean percentage of glial cells density. The results of glial cell quantification along the 4900-μm long spinal cord (including the gray and white matter of the injured spinal cord) showed a
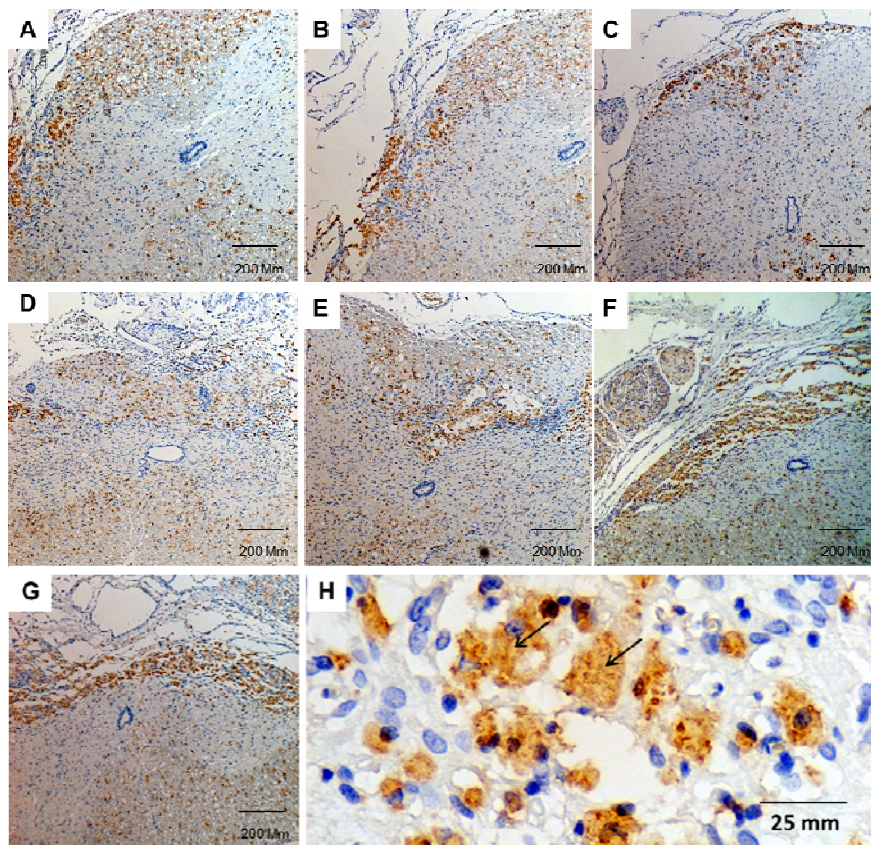
Fig. 1. ED-1 immunoreactivity in the lesion site of a contused spinal cord at various time points. **(A–G)** represent photomicrographs showing an increase in the density of ED-1 positive cells at day 1 (A), day 2 (B), day 4 (C), week 1 (D), week 2 (E), week 3 (F), and week 4 (G) after SCI; **(H)** represents ED-1 positive cells. Brown colors represent the immunopositive site, whereas blue colors represent hematoxylin staining. Black arrows indicate ED-1 immunoreactive cells.

significant increase in glial cell density percentage at day 2 (85.45 ± 3.71) as compared to that at days 1 and 4 as well as weeks 1, 2, 3, and 4 (81.06 ± 2.39, 66.71 ± 6.99, 56.17 ± 4.56, 45.80 ± 10.87, 47.94 ± 13.89 and 48.37 ± 3.53, respectively) post injury. Data analyses are shown in Figures 3 and 4.

Cavitation analyses. Mean cavity percentages were assessed by evaluating the histological sections obtained during 28 days after the injury. The mean cavity percentage of the 4900-μm long injured spinal cord was evaluated using the image J software. There were significant differences among the groups. The mean cavity percentage at week 3 was 8.88 ± 0.98 and that at weeks 4, 1, and 2 was 18.65 ±1.8, 2.1 ± 0.69, and 3.85 ± 0.55, respectively. Moreover, we noticed a significant difference between weeks 3 and 4 post injury groups. Data analyses are presented in Figures 5 and 6.

DISCUSSION

This study provides a new insight into the immune response to SCI, including cellular inflammation,

macrophages/microglia activation, glial cell density, and cavitation. Taken together, our finding indicates that a multiphasic response of cellular inflammation is observed after SCI.
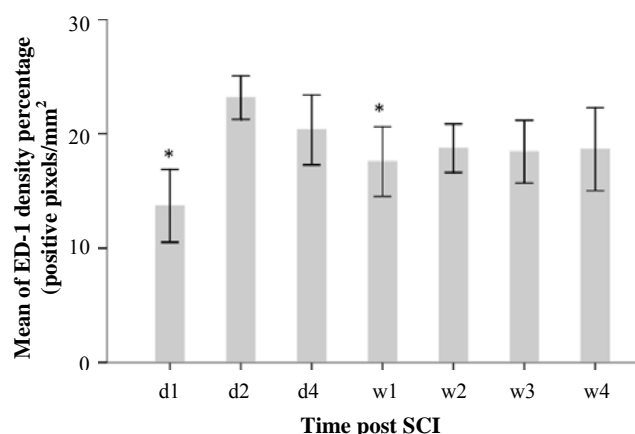

Fig. 2. A histogram of ED-1 immunoreactivity constructed using densitometry of brown color pixels per square millimeter (pixel intensity/mm^2) at different time points [days 1, 2, and 4 and weeks 1, 2, 3, and 4] after injury. A significant difference was observed between day 1 and week 1 groups as compared to that between day 1 and day 2 group (*$P<0.05$). d, day; w, week
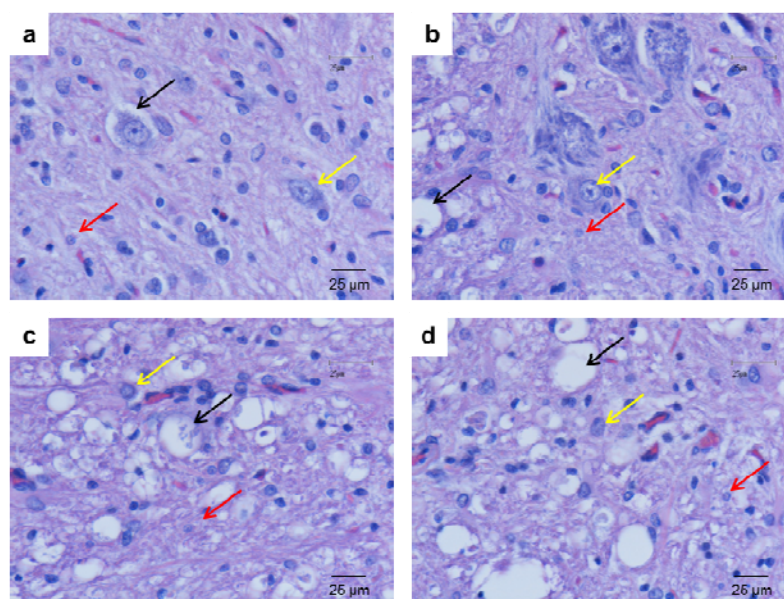
Fig. 3. Photomicrographs of the ventral horn of the contused spinal cord stained with routine stains (H & E). Glial cell density was evaluated at week 1 (**A**), week 2 (**B**), week 3 (**C**), and week 4 (**D**) after injury. Black, red, and yellow arrows represent vacuolization of dead cells, glial cells, and motor neuron, respectively.

We used contusion rat SCI model, morphometry, and immunostaining to assess the response of glial cell types and macrophages/microglia activation at different time points. Inflammatory response after traumatic SCI is primarily due to the disruption of the blood-spinal cord barrier, followed by the release of pro-inflammatory cytokines and upregulation of adhesion molecules in the vascular endothelium [19]. These events lead to the infiltration of monocytes, lymphocytes, and macrophages into the damaged site [20]. Inflammatory response can lead to axon demyelination and neuroglial apoptosis with subsequent loss of neurological function [21]. Between 3-24 hours post injury, proinflammatory cytokines such as TNF-α and IL-6 are upregulated around the lesion area [22], resulting in a 6-fold increase in the number of neutrophils [23].

Furthermore, activated microglia and resident macrophages can evoke a response (Chemokines initiate activation and migration of microglia) [24]. Resident microglia rapidly respond to the microenvironment by changing their morphology, expression of specific cell surface molecules, and release of cytokines such as IL-1, and TNF-α, and chemokines such as leukotrienes and prostaglandins [25, 26, 7]. Large numbers of activated resident microglia and invading peripheral macrophages can be soon observed after injury and persist for several weeks
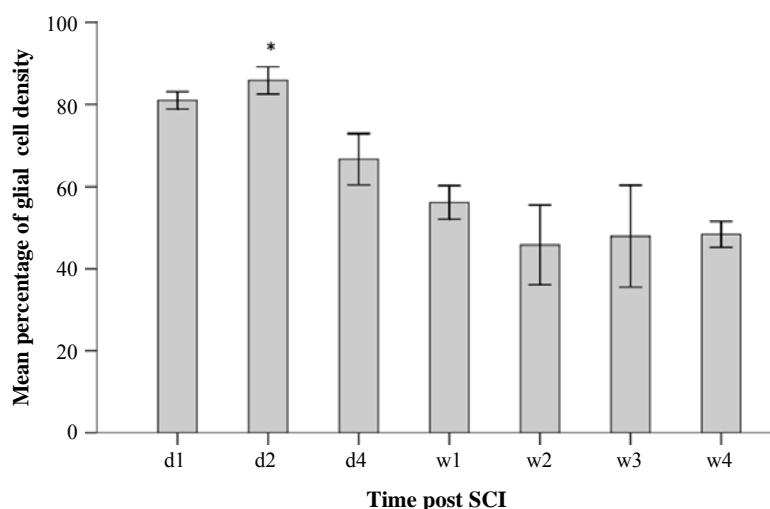

Fig. 4. A histogram of mean glial cell density percentage of the injured spinal cord during 28 days after injury. * represents the significance level with other groups ($P<0.05$). d, day; w, week
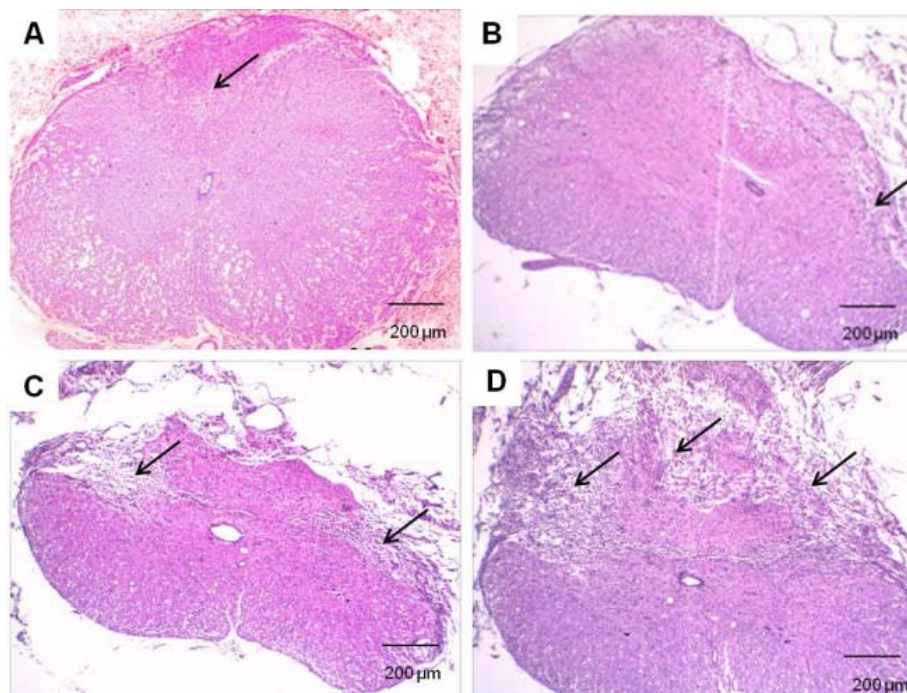
Fig. 5. Routine staining (H & E) of contused spinal cord in rats. Evaluation of cavity percentage in gray and white matter at week 1 (**A**), week 2 (**B**), week 3 (**C**), and week 4 (**D**) after injury. Black arrows indicate cavity formation.

[27]. Influx of macrophages derived from microglia probably starts very soon after injury, whereas active migration of hematogenous macrophages is slightly delayed and is reported to start 3 days after injury in rats [27, 19].

Several studies have shown a time-dependent distribution of immune cells in the injured cord tissue [28- 30]. In this study, assessment of ED-1 positive cells in the injured spinal cord was performed across multiple time points for the first 7 days and then weekly for up to 4 weeks. We found that during earlier hours (3 - 48 h) after injury, ED-1 positive cells were dispersed; however, in the sub-acute phase, these cells

Fig. 6. Mean cavity percentage of the 4900-µm long injured spinal cord during 28 days after injury. *represents the significance level with other groups ($P<0.05$).

low numbers of ED-1 positive cells were observed between days 7 and 14 (lowest at day 7 after SCI). This result is consistent with that of other investigative reports [14, 27]. We observed an increase in the number of activated macrophages/microglia (ED-1 positive cells) on day 2 after injury as compared to that at other times points. The number of ED-1 positive cells was lowest on day 7 after injury, suggesting a clear division between the phases of inflammation. No significant changes were observed in the number of ED-1 positive cells during the subacute phase.

Macrophages have been proposed to participate in tissue destruction, cavity enlargement, and secondary pathological response [31]. After SCI, some cells at the lesion site die because of post-traumatic necrosis, whereas others die because of apoptosis [32]. Therefore, cell death of both neurons and oligodendrocytes may greatly contribute to paralysis in patients with SCI [33].

In conclusion, better understanding of the inflammatory processes associated with acute SCI would permit the development of better therapeutic strategies. Our results and the results of previous studies suggest that cellular inflammation has complex, time-dependent functions. Understanding the role of multiphasic response after SCI provides new insights for designing rational therapeutic strategies and determining the optimal time for cell transplantation and pharmaceutical treatment.
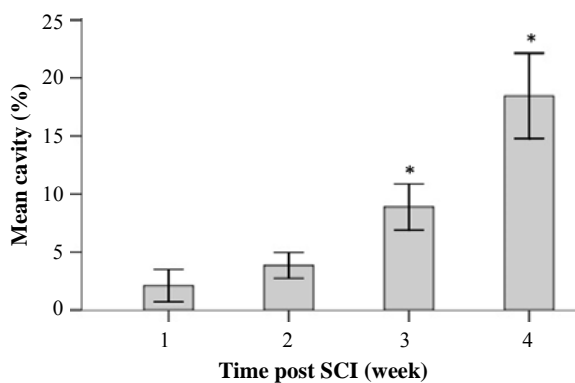
REFERENCES

1. Hyun JK, Kim HW. Clinical and experimental advances in regeneration of spinal cord injury. *J Tissue Eng. 2010 Nov 2;2010:650857.*

2. Hawryluk GW, Rowland J, Kwon BK, Fehlings MG. Protection and repair of the injured spinal cord: a review of completed, ongoing, and planned clinical trials for acute spinal cord injury. *Neurosurg Focus. 2008;25(5):E14.*

3. Whalley K, O'Neill P, Ferretti P. Changes in response to spinal cord injury with development: vascularization, hemorrhage and apoptosis. *Neuroscience. 2006 Feb;137(3):821-32.*

4. Hausmann ON, Hu WH, Keren-Raifman T, Witherow DS, Wang Q, Levay K, et al. Spinal cord injury induces expression of RGS7 in microglia/macrophages in rats. *Eur J Neurosci. 2002 Feb;15(4):602-12.*

5. Hayashi M, Ueyama T, Nemoto K, Tamaki T, Senba E. Sequential mRNA expression for immediate early genes, cytokines, and neurotrophins in spinal cord injury. *J Neurotrauma. 2000 Mar;17(3):203-18.*

6. Tian DS, Xie MJ, Yu ZY, Zhang Q, Wang YH, Chen B, et al. Cell cycle inhibition attenuates microglia induced inflammatory response and alleviates neuronal cell death after spinal cord injury in rats. *Brain Res. 2007 Mar;1135(1):177-85.*

7. Popovich PG, Wei P, Stokes BT. Cellular inflammatory response after spinal cord injury in Sprague-Dawley and Lewis rats. *J Comp Neurol. 1997 Jan; 377(3):443-64.*

8. Glauben R, Batra A, Fedke I, Zeitz M, Lehr HA, Leoni F, et al. Histone hyperacetylation is associated with amelioration of experimental colitis in mice. *J Immunol. 2006 Apr; 176(8):5015-22.*

9. Carlson SL, Parrish ME, Springer JE, Doty K, Dossett L. Acute inflammatory response in spinal cord following impact injury. *Exp Neurol. 1998 May;151(1):77-88.*

10. Beattie MS, Li Q, Bresnahan JC. Cell death and plasticity after experimental spinal cord injury. *Prog Brain Res. 2000;128:9-21.*

11. Kearney PA, Ridella SA, Viano DC, Anderson TE. Interaction of contact velocity and cord compression in determining the severity of spinal cord injury. *J Neurotrauma. 1988; 5(3):187-208.*

12. Agrawal G, Kerr C, Thakor NV, All AH. Characterization of graded multicenter animal spinal cord injury study contusion spinal cord injury using somatosensory-evoked potentials. Spine (Phila Pa 1976). *2010 May 15; 35(11):1122-7.*

13. Khalatbary AR, Tiraihi T. Localization of bone marrow stromal cells in injured spinal cord treated by intravenous route depends on the hemorrhagic lesions in traumatized spinal tissues. *Neurol Res. 2007 Jan; 29(1):21-6.*

14. Llewellyn BD. Nuclear staining with alum hematoxylin. *Biotech Histochem. 2009; 84(4):159-77.*

15. Michel RP, Cruz-Orive LM. Application of the Cavalieri principle and vertical sections method to lung: estimation of volume and pleural surface area. *J Microsc. 1988 May;150(Pt 2):117-36.*

16. Reichenbach A, Siegel A, Rickmann M, Wolff JR, Noone D, Robinson SR. Distribution of Bergmann glial somata and processes: implications for function. *J Hirnforsch. 1995; 36(4):509-7.*

17. Barakat L, Bordey A. GAT-1 and reversible GABA transport in Bergmann glia in slices. *J Neurophysiol. 2002 Sep; 88(3):1407-19.*

18. McLaren JW, Bourne WM, Patel SV. Automated assessment of keratocyte density in stromal images from the ConfoScan 4 confocal microscope. *Invest Ophthalmol Vis Sci. 2010 Apr; 51(4):1918-26.*

19. Hausmann ON. Post-traumatic inflammation following spinal cord injury. *Spinal Cord. 2003 Jul;41(7):369-78.*

20. Pineau I, Sun L, Bastien D, Lacroix S. Astrocytes initiate inflammation in the injured mouse spinal cord by promoting the entry of neutrophils and inflammatory monocytes in an IL-1 receptor/MyD88-dependent fashion. *Brain Behav Immun. 2010 May;24(4):540-53.*

21. Liu H, Shubayev VI. Matrix metalloproteinase-9 controls proliferation of NG2+ progenitor cells immediately after spinal cord injury. *Exp Neurol. 2011 Oct;231(2):236-46.*

22. Habgood MD, Bye N, Dziegielewska KM, Ek CJ, Lane MA, Potter A, et al. Changes in blood-brain barrier permeability to large and small molecules following traumatic brain injury in mice. *Eur J Neurosci. 2007 Jan; 25(1):231-8.*

23. Fu ES, Saporta S. Methylprednisolone inhibits production of interleukin-1beta and interleukin-6 in the spinal cord following compression injury in rats. *J Neurosurg Anesthesiol. 2005 Apr;17(2):82-5.*

24. Grimpe B, Silver J. The extracellular matrix in axon regeneration. *Prog Brain Res. 2002;137:333-49.*

25. Streit WJ, Graeber MB, Kreutzberg GW. Functional plasticity of microglia. *Glia.1988;1(5):301-7.*

26. Trivedi A, Olivas AD, Noble-Haeusslein LJ. Inflammation and Spinal Cord Injury: Infiltrating Leukocytes as Determinants of Injury and Repair Processes. *Clin Neurosci Res. 2006 Dec;6(5):283-292.*

27. Saville LR, Pospisil CH, Mawhinney LA, Bao F, Simedrea FC, Peters AA, et al. A monoclonal antibody to CD11d reduces the inflammatory infiltrate into the injured spinal cord: a potential neuroprotective treatment. *J Neuroimmunol. 2004 Nov;156(1-2):42-57.*

28. Nguyen HX, Beck KD, Anderson AJ. Quantitative assessment of immune cells in the injured spinal cord tissue by flow cytometry: a novel use for a cell purification method. *J Vis Exp. 2011; 9: 50.*

29. Beck KD, Nguyen HX, Galvan MD, Salazar DL, Woodruff TM, Anderson AJ. Quantitative analysis of cellular inflammation after traumatic spinal cord injury: evidence for a multiphasic inflammatory response in the

acute to chronic environment. *Brain. 2010; 133(Pt 2):433-47.*

30. Dunn EA, Weaver LC, Dekaban GA, Foster PJ. Cellular imaging of inflammation after experimental spinal cord injury. *Mol Imaging. 2005; 4(1):53-62.*

31. Glaser J, Gonzalez R, Sadr E, Keirstead HS. Neutralization of the chemokine CXCL10 reduces apoptosis and increases axon sprouting after spinal cord injury. *J Neurosci Res. 2006 Sep;84(4):724-34.*

32. Byrnes KR, Stoica BA, Fricke S, Di Giovanni S, Faden AI. Cell cycle activation contributes to post-mitotic cell death and secondary damage after spinal cord injury. *Brain. 2007 Nov;130(Pt 11):2977-92.*

33. Mattson MP. Apoptosis in neurodegenerative disorders. *Nat Rev Mol Cell Biol. 2000 Nov;1(2):120-9.*